

Time-temperature effects in dual scale crack growth of titanium alloys

K.K.Tang^aZ.Q.Wang^aF.Berto^b

<https://doi.org/10.1016/j.tafmec.2017.06.016>Get rights and content

Abstract

Time and temperature effects play substantial role in the microstructural degradation of metal materials. There results in complex creep-fatigue interaction. The explicit representation of material damage is preferably assumed to be a characteristic length such as an equivalent crack length. A dual scale crack growth model that is based on the theory of strain energy density is employed to study the time-temperature effects on the crack growth behaviors of titanium alloys. Three micro/macro parameters defined in the model are used to exhibit the time-dependent variation of material, loading and geometry effects. TA7 and TA19 of titanium alloys are used to particularly address the effects of temperature variation as well as scale parameters. The numerical results show the microscopic Poisson's ratio is sensitive to the crack growth history of titanium alloys. The inverse approach of creep-fatigue cracking can be possibly applied to the health monitoring of crack growth in fracture control.

Keywords

Time-temperature effects

Dual scale model

Creep-fatigue interaction

Titanium alloys

Crack growth

1. Introduction

Creep-fatigue interaction is a [complex process](#) of damage involving creep deformation as well as [cyclic stress](#). At high temperature, [substantial damage](#) can be caused by creep in metal alloys over a [long period](#) of time. When the level of [applied stress](#) is getting higher, there inevitably arises fatigue in underlying materials. The process of creep-fatigue interaction is alternatively mechanical and thermal, and equally significant. Unfortunately to these days, the accompanying [failure mechanisms](#) of creep and fatigue is still unclear.

It is generally accepted that temperature and time-dependent material properties are the critical issues to be addressed in the process of creep-fatigue interaction [1].

Microscopic and [macroscopic](#) parameters thus need to be defined to clarify the dual mechanism interactions, which leads to the multiscaling approach [2], [3], [4], [5], [6] introduced to the solution of creep and fatigue. Multiscaling approach offers an innovative perspective, recognizing that [smaller scale](#) such as micro effects need to be considered as well as macro effects. Energy criterion is flexible in multiscaling problems. There are cyclic [hysteresis energy](#) as well as [strain energy density](#). Hysteresis energy exerts physical explanation for material failure, thus is more sensitive to small changes of the prediction parameters. [Fatigue crack initiation and propagation](#) is studied by using hysteresis energy criterion in [7]. It is emphasized that the hysteresis energy criterion is combined with continuum damage modelling, therefore it is able to study the [material degradation](#) at the microstructural level. [Strain energy density criterion](#) [8], [9] is an [effective approach](#) when it comes to assessment of the severity of material degradation such as creep-fatigue interaction. It is commonly recognized that the simple and straightforward damage representation would be a characteristic length such as an equivalent [crack length](#). Theory of SED is practical to the explicit representation of multiscaling material damage degradation. It is defined as the strain energy stored in a [volume element](#) ahead of a [crack tip](#) that is a quadratic form of stresses. The energy density factor S is treated as the released energy at the initiation of instability and serves as a [crack growth](#) factor in fatigue. It is applied to multiscaling problems, including [fatigue assessment](#) of cracks and notches [10], [11], [12], [13], [14], [15], and further [engineering components](#) and structures [16], [17].

It shall be noticed the SED approach is employed to the assessment of thermal and [residual stresses, quantification](#) of the influence of residual stresses on [fatigue strength](#) of [Al alloy](#) welded joints is studied in [18], [19], [20]. This approach provides an innovative tool for evaluation of the thermal-mechanical behaviors in critical engineering materials and components.

Recent advances on multiscaling offer new perspective on creep-fatigue interaction. A dual scale micro/macro crack growth model is developed in [2], [3], [4] such that the scale transitory behaviors can be best reflected, where weak and strong singularities correspond to distinctive [scale ranges](#). Three micro/macro- parameters are defined to reflect material, loading and geometry effects on fatigue [crack growth behaviors](#). Furthermore, the implicit character of microstructural degradation is discussed by specifying the [time history](#) of crack growth caused by creep-fatigue interaction at high

temperature. An ultra-high [strength steel](#) 38Cr2Mo2VA is considered in high temperature environment [1]. Compared to ultra-high strength steel, [titanium alloys](#) have high [strength to weight ratio](#) and excellent [corrosion resistance](#), being capable of withstanding extreme temperatures. The [time-temperature](#) effects on creep-fatigue interaction are distinctively different from those of ultra-high strength steels. The thermal-mechanical creep and fracture crack growth of a near-alpha titanium alloy TA12 are investigated in [21]. Influences of [temperature profiles](#) and perturbation number on [crack growth history](#) are emphasized. Nevertheless, some of the critical issues such as time-temperature [dependent material](#) properties remains unclear to titanium alloys. This paper aims to focus on the aspect of microstructural degradation in TA7 and TA19 of titanium alloys. Discussed are the effects of temperature profiles and microscopic material properties on crack growth history of titanium alloys.

2. Thermal-mechanical dual scale crack growth model

Creep and fatigue interaction can be treated as the exchange of thermal and mechanical energy. The inherent coupling mechanism of heat and work is one of most complex [physical phenomena](#) that still need to be clarified. It is postulated that thermal loading to [thermal effects](#) is equivalent to [mechanical loading](#) to mechanical effects. Therefore they do not interact and are interchangeable.

2.1. Dual scale crack growth relation

A dual [crack growth](#) model was formulated in previous work [2], [3], [4]. Similar to the conventional [crack growth rate](#) model, the crack growth rate can be expressed for the dual [scale model](#) as:

$$(1) \frac{da}{dt} = \psi \Delta S_{\text{micro}} \phi$$

in which ψ and ϕ are two scale sensitive floating parameters. Selection of the two scale parameters depends on the initial size of the equivalent half-crack length a . Compared to conventional increment of [stress intensity factor](#) ΔK , ΔS_{micro} is the [incremental](#) energy density factor that incorporates both [micro-cracks](#) and macro-cracks in the physical process of [material degradation](#). It is further elaborated as

$$(2) \Delta S_{\text{micro}} = 2(1 - 2\nu_{\text{micro}})(1 - \nu_{\text{macro}})^2 \sigma \sigma_{\text{micro}} \mu^* (1 - \sigma^*)^2 d^*$$

where the three normalized generic parameters are defined to reflect the effects of material, loading and geometry, respectively. Note that ν_{micro} and ν_{macro} represent microscopic and [macroscopic](#) Poisson's ratio.

$$(3) \mu^* = \mu_{\text{micro}} \mu_{\text{macro}}, \sigma^* = \sigma / \sigma_{\infty}, d^* = d / d_0$$

where μ_{macro} is macroscopic [shear modulus](#) and μ_{micro} microscopic shear modulus, being σ_0 microscopically restraining stress and σ^∞ macroscopically [applied stress](#). σ_a and σ_m are two ordinary parameters as [stress amplitude](#) and mean stress. d and d_0 respectively stand for the notch depth and the grain size of specific metal alloy. r is the [scale distance](#) parameter that reflects the local and global behavior of crack growth.

2.2. Exchange of creep and fatigue – perturbation index

Specific perturbation index η shall be defined to reflect the exchange of creep and fatigue interaction. The product relationship $\sigma_a \sigma_m$ incorporated in the increment change of the energy density factor $\Delta S_{\text{micro/macro}}$ is the reflection of creep and fatigue interaction. A perturbation parameter η shall be defined as

$$(4) \sigma_{\text{max}} = \sigma, \sigma_{\text{min}} = \eta \sigma$$

The stress amplitude and mean stress then can be rewritten as a function of [maximum stress](#) amplitude σ_{max} and minimum stress amplitude σ_{min}

$$(5) \sigma_a = \frac{\sigma_{\text{max}} - \sigma_{\text{min}}}{2} = 1 - \eta \frac{\sigma_{\text{max}} + \sigma_{\text{min}}}{2} = 1 - \eta \sigma_m$$

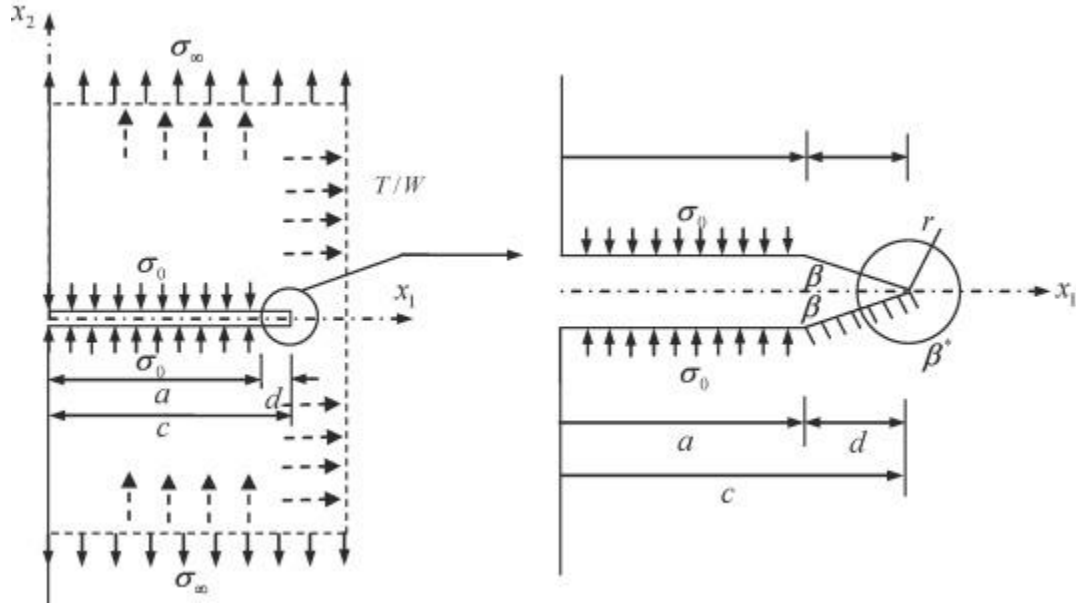
It is observed in Eq. (5) that variation of perturbation parameter η results in the variation of product $\sigma_a \sigma_m$, consequently affects the crack growth rate. $\eta=1$ indicates maximum stress is equal to minimum stress, which results in the case when creep under constant load. While η is taken as -1 , the [extreme case](#) would be $\sigma_{\text{max}} = -\sigma_{\text{min}}$, the stress would alternate between tension and [compression load](#) with zero mean stress. This would be the extreme effect of fatigue. In most cases, creep and fatigue would both occur.

2.3. Thermal-mechanical exchange in dual scale model

Assumption is made that thermal and [mechanical loads](#) are interchangeable without interaction, refer to [Fig. 1](#). The mechanical applied stress may be treated as a [thermal gradient](#) expressed by [1]

$$(6) \sigma(T) = \alpha E_{\text{macro}} \frac{1}{4(1-\nu_{\text{macro}})} T w$$

where α is the thermal [coefficient of linear expansion](#), T is temperature field that is a [function of time](#) t . W is the width of the panel plate. More details about the model can be found in Ref. [1].



1. [Download high-res image \(173KB\)](#)
2. [Download full-size image](#)

Fig. 1. Thermal-mechanical dual scale [crack growth](#) model [1].

By combining Eqs. (2), (3), (4), (5), (6), the incremental [strain energy density](#) factor $\Delta S_{micromacro}$ can be further expressed as

$$(7) \Delta S_{micromacro} = (1 - \eta_2)(1 + \nu_{macro})(1 - 2\nu_{micro}) \alpha^2 E_{macro} \frac{1}{16} (T/W)^2 a^3 \mu^* (1 - \sigma^*)^2 d^* \text{dor}$$

Refer to Eq. (1), There results in the derivative form of crack growth rate:

$$(8) \frac{da}{dt} = \psi (1 - \eta_2)(1 + \nu_{macro})(1 - 2\nu_{micro}) \alpha^2 E_{macro} \frac{1}{16} (T/W)^2 a^3 \mu^* (1 - \sigma^*)^2 d^* \text{dor} \phi$$

Through [numerical integration](#), the [time history](#) of crack growth $a(t)$ can be generated, without loss for generality, $\phi = 1$ is considered here,

$$(9) \Delta a_i = \psi (1 - \eta_2)(1 + \nu_{macro})(1 - 2\nu_{micro}) \alpha^2 E_{macro} \frac{1}{16} T_w^2 a_i^{1-3} \mu^* (1 - \sigma^*)^2 d^* \text{dor} \Delta t$$

and

$$(10) a_i = a_{i-1} + \Delta a_i$$

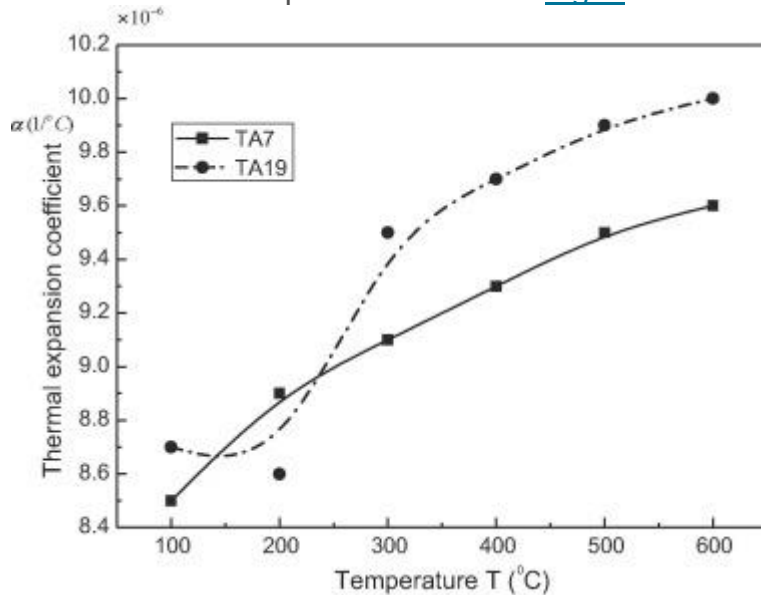
Notice scale parameter ψ in Eq. (9) is determined by the [desired time](#) of material. Thus an inverse approach is taken and this will be further discussed in the following sections.

3. Time-temperature effects in material degradation of titanium alloys

TA7 and TA19 of [titanium alloys](#) are used to demonstrate the [time-temperature](#) effects in [material degradation](#). The time and temperature degradation of micro/macro parameters are addressed through this section.

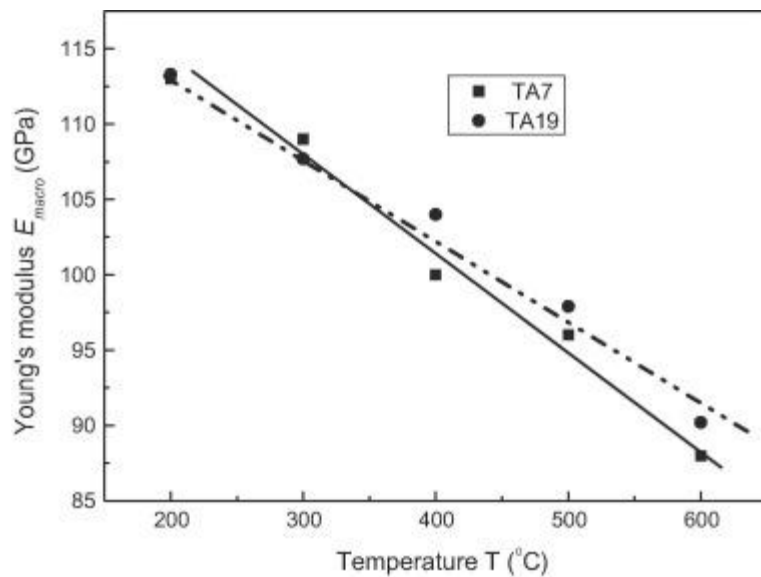
3.1. Temperature-dependent materials properties of titanium alloys

TA7 and TA19 of titanium alloys are selected for their distinctive differences in micro/macro parameters. Based on the test data [22], thermal expansion coefficient α , macroscopic material properties including Young's modulus and Poisson's ratio of TA7 and TA19 are displayed in Fig. 2, Fig. 3, Fig. 4. Basically, the numerical values are decreasing over the rise of temperature approximately from 20 °C to 600 °C. It shall be pointed out that the numerical values of Poisson's ratio of TA7 are increasing over the rise of temperature. Refer to Fig. 4 for the contrasting trend of TA7 and TA19.



1. [Download high-res image \(119KB\)](#)
2. [Download full-size image](#)

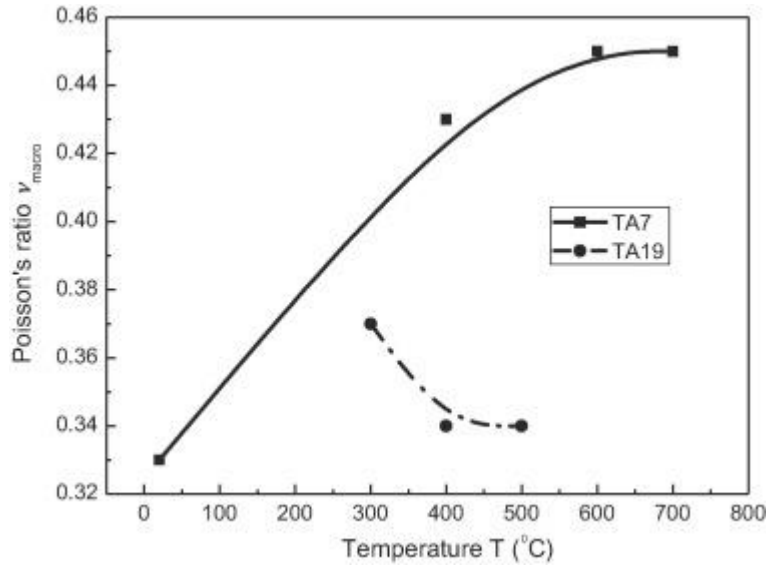
Fig. 2. Thermal expansion coefficient α versus temperature T [22].



1. [Download high-res image \(108KB\)](#)

2. [Download full-size image](#)

Fig. 3. Young's modulus E_{macro} versus temperature T [22].



1. [Download high-res image \(107KB\)](#)

2. [Download full-size image](#)

Fig. 4. Poisson's ratio v_{macro} versus temperature T [22].

Based on test data for thermal expansion coefficient α of TA7 and TA19, there results in the following fitting equation

$$(11) \alpha_1(T) = 8.033 \times 10^{-6} + 5.485 \times 10^{-9}T - 7.54 \times 10^{-12}T^2 + 4.63 \times 10^{-15}T^3$$

$$\alpha_2(T) = 1.71 \times 10^{-5} - 1.702 \times 10^{-7}T + 1.17 \times 10^{-9}T^2 - 3.55 \times 10^{-12}T^3$$

Refer to [Fig. 2](#) for the [graphical representation](#). Unit of temperature T is [Celsius degree](#). Notice the [subscript](#) 1 and 2 stand for TA1 and TA19, respectively. Same can be done to macroscopic material properties such as Young's modulus for TA7 and TA19. [Linear functions](#) are listed as follows

$$(12) E1_{macro}(T) = 126.4 - 0.063T$$

$$E2_{macro}(T) = 119.4 - 0.051T$$

Notice the unit of Young's modulus is GPa. Refer to the curves in [Fig. 3](#) for Young's modulus variation over temperature range.

$$(13) v1_{macro}(T) = 0.322 + 0.0000385846T - 2.90061 \times 10^{-7}T^2$$

$$v2_{macro}(T) = 0.64 - 0.00135T + 1.5 \times 10^{-6}T^2$$

Refer to the graph in [Fig. 4](#) for the comparison of Poisson's ratio for TA7 and TA19.

In Eq. [\(9\)](#), there still remains ψ to be determined. Scale parameter ψ is empirically determined as the y-intercept when using the two-parameter [fatigue crack](#)

[growth](#) relation in log-log plots. A linear function is assumed for the decaying evolution over temperature as

$$(14) \psi = \psi_0 (1.2 - 0.00064T) \quad \psi_0 = 5.0 \times 10^2 \text{ mm}^2 / (\text{Nyr})$$

Keep in mind that ψ is related to the initial size [crack length](#) a . ψ_{micro} corresponds to microscopic crack length. ψ_0 in the present work is used to satisfy the design of 10-year requirement.

3.2. Time-dependent material properties of titanium alloys

Materials age over time. Material degradation are irreversibly caused by time and [environmental loads](#). [Physical parameters](#) α , E_{macro} , and v_{macro} should vary with both temperature and time. Therefore, the following analytical assumption is given

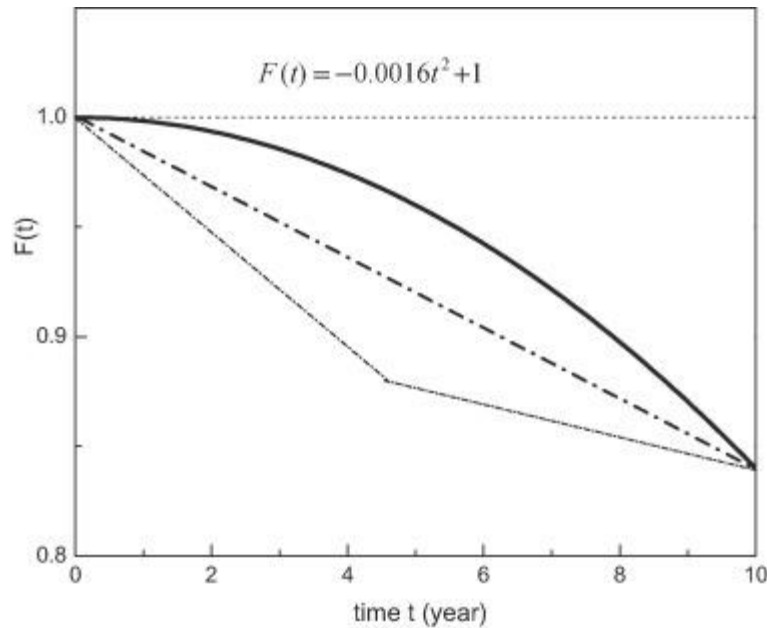
$$(15) \alpha(T, t) = \alpha(T) F_\alpha(t) \quad E_{\text{macro}}(T, t) = E_{\text{macro}}(T) F_E(t) \quad v_{\text{macro}}(T, t) = v_{\text{macro}}(T) F_v(t),$$

The following condition should be satisfied for aging function:

$$(16) 0 \leq F(t) \leq 1$$

Choice of the aging functions $F_\alpha(t)$, $F_E(t)$, and $F_v(t)$ shall follow the aging process which is supposed to be slow at the beginning and fast at the end. The precise expression of decaying function remains unknown. In [Fig. 5](#), assumed are three curves of aging function. It is commonly postulated that the parabola line instead of [straight line](#) or polyline relatively tally with the process of material degradation. The coefficients of these functions are determined approximately from the desired life expectancy. For simplicity, the same parabola curve for above parameters in the aging process is adopted and expressed as [Fig. 5](#)

$$(17) F(t) = -0.0016t^2 + 1$$



1. [Download high-res image \(107KB\)](#)
2. [Download full-size image](#)

Fig. 5. Decaying function of $F(t)$.

Refer to [Fig. 5](#) for the graphical representation of aging process. Assume variation of ψ be negligible. Combination of Eqs. [\(11\)](#), [\(12\)](#), [\(13\)](#), [\(15\)](#), [\(16\)](#) results in the macroscopic material properties related to temperature and time.

3.3. Time-dependent scale parameters

Microscopic material properties cannot be achieved through [specimen test](#). However, they can be analytically evaluated through scale parameters σ^* , μ^* , and d^* . An inverse approach is taken. Thus 10 years of [design requirement](#) needs to be satisfied, the [time decay](#) of σ^* , μ^* , and d^* shall be connected with the [design criterion](#). The [crack growth](#) in relation to the [time history](#) of the micro-structural degradation are accounted by σ^* , μ^* , and d^* . They are a [function of time](#).

Based on the inverse principle and 10 years of design requirement, the time decay of σ^* , μ^* , and d^* will be expressed as a function of time t . Following the rule that the aging process is basically slow at the beginning and speeds up in the end. Without going into the details, three decaying function are selected as

$$(18) \sigma^*(t) = -0.004t^2 + 0.5 \mu^*(t) = 0.002t^2 - 0.05t + 3 d^*(t) = -0.01t^2 + 5$$

A fictitious ν_{micro} shall be defined to relate μ_{micro} to E_{micro} and complete the set of microscopic material properties. A microscopic Poisson's ratio ν_{micro} relation is assumed to be

$$(19) v_{\text{micro}}(T, t) = v^*(t) v_{\text{macro}}(T)$$

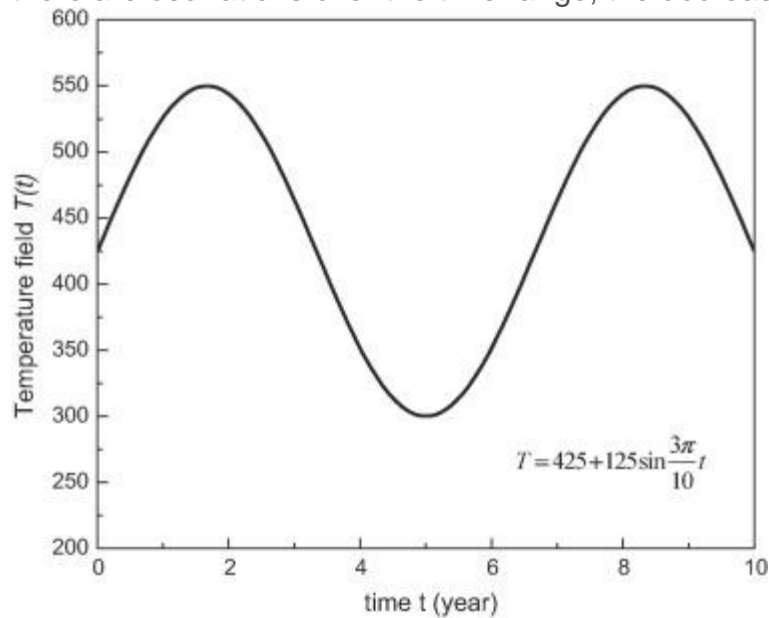
Macroscopic Poisson's ratio can be found in Eq. (13) and Fig. 4. Unlike other microscopic material properties, the following $v^*(t)$ is taken as

$$(20) v_1^*(t) = -0.005t^2 + 1.12 \quad v_2^*(t) = -0.0035t^2 + 1.3$$

In the following discussion, temperature field is set to be

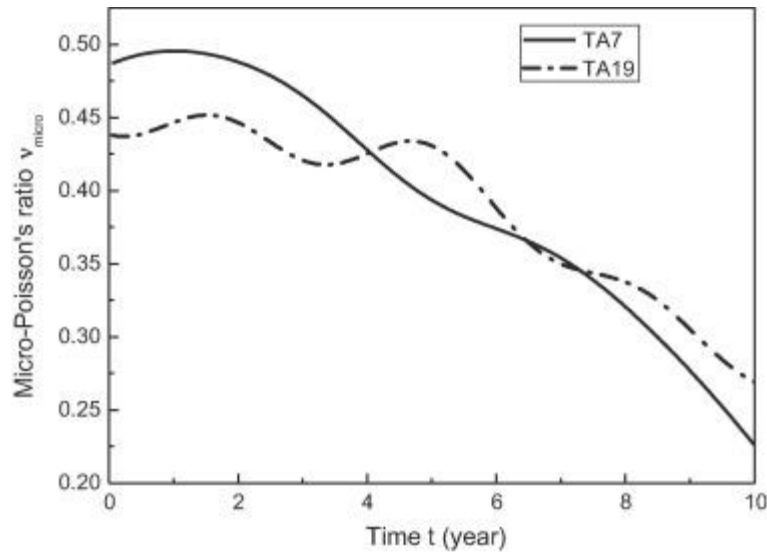
$$(21) T(t) = 425 + 125 \sin 3\pi 10t$$

Refer to Fig. 6 for the [temperature change](#) over a period of 10 years. Notice temperature field T is a function of time t (year). Combination of Eqs. (13), (19), (20), (21) gives rise to the curve of microscopic Poisson's ratio v_{micro} versus time t . The curves are displayed in Fig. 7. It is observed that difference between the two curves is appreciable. This is attributed to the disparately variation of macroscopic Poisson's ratio over the range of temperature field. Though there are oscillations over the time range, the decreasing trend of curve remains clear.



1. [Download high-res image \(105KB\)](#)
2. [Download full-size image](#)

Fig. 6. [Sinusoidal variation](#) of temperature field.



1. [Download high-res image \(103KB\)](#)
2. [Download full-size image](#)

Fig. 7. Fictitious micro-Poisson's ratio v_{micro} versus time.

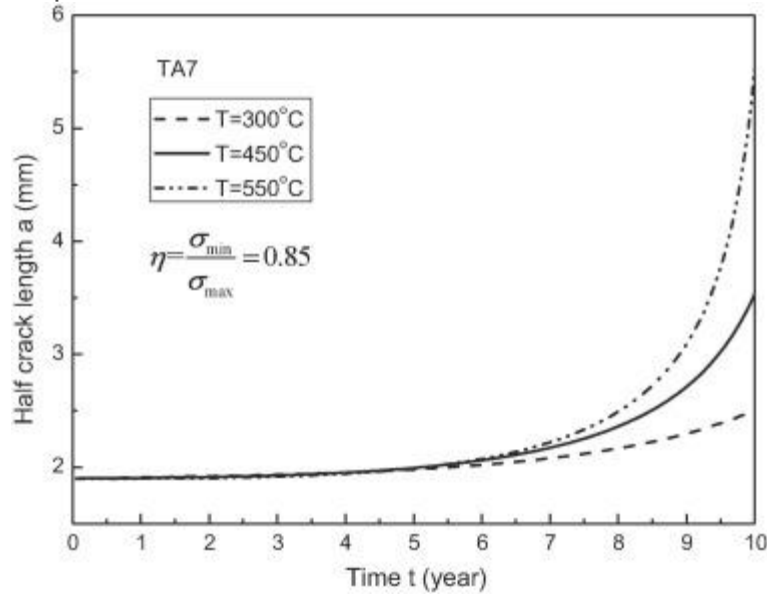
4. Results and discussions

The integration of Eq. (9) results in the half [crack length](#) a . The perturbation index η is taken as 0.85 in the following cases. It is creep-fatigue interaction where both creep and fatigue would occur. Relatively speaking, $\eta=0.85$ indicates higher mean stress and smaller [stress amplitude](#). There creep prevails over fatigue. [Temperature profiles](#), microscopic [Poisson' ratio](#) as well as material difference of TA7 and TA19, are respectively discussed in this section.

4.1. Crack growth history influenced by extreme temperatures

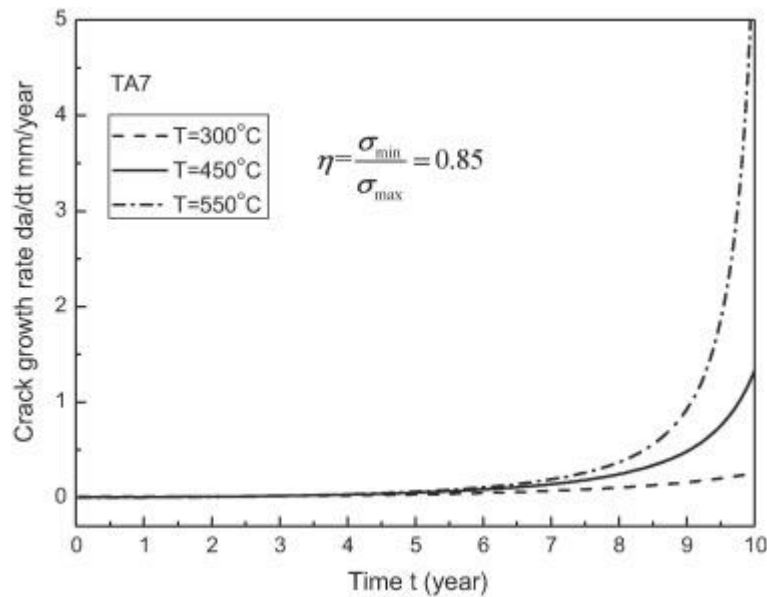
The extreme temperature designed for TA7 and TA12 of [titanium alloys](#) is 550 °C, which means titanium alloys is able to withstand long [operating hours](#) of high temperature up to 550 °C. Let the temperature remains unchanged at 300 °C, 400 °C and 550 °C for TA7, respectively. The [initial crack length](#) is 1.9 mm. Influence of constant temperature on [crack growth behaviors](#) are displayed in [Fig. 8](#), [Fig. 9](#). When the temperature is relatively low, say at 300 °C, the crack length after 10 years is not bigger than 2.5 mm. The [crack growth rate](#) remains steadily increasing. The medium temperature profile of 400 °C leads to a rapid increase of crack length and [crack growth](#) rate, compared to that of 300 °C. However, it still meets the requirement of 10 years of [life design](#). An extreme constant temperature of 550 °C makes the appearance of critical crack length approximately at 9 years. It barely meets 10 years of design for titanium alloys of TA7.

Even for the [initial crack size](#) of 1.9 mm, extreme temperature shall be avoided as much as possible.



1. [Download high-res image \(107KB\)](#)
2. [Download full-size image](#)

Fig. 8. Constant temperature field: Half [crack length](#) a versus time t .

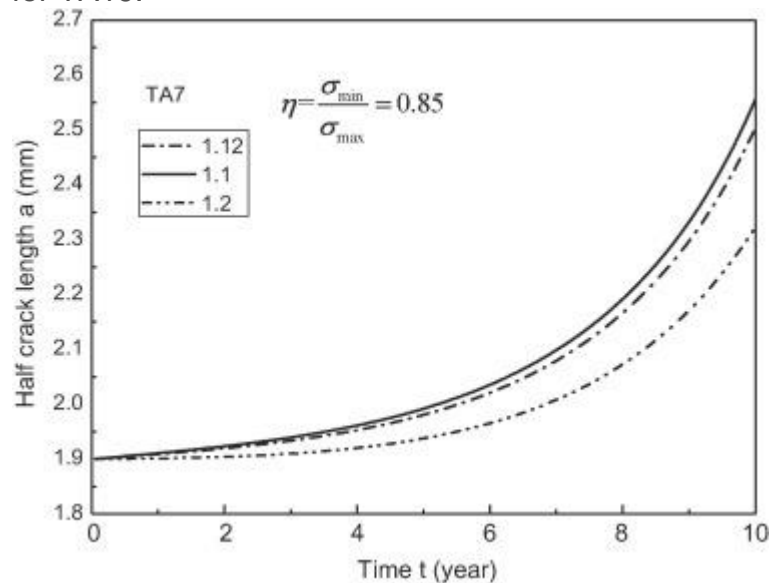


1. [Download high-res image \(108KB\)](#)
2. [Download full-size image](#)

Fig. 9. Constant temperature field: [Crack growth rate](#) da/dt versus time t .

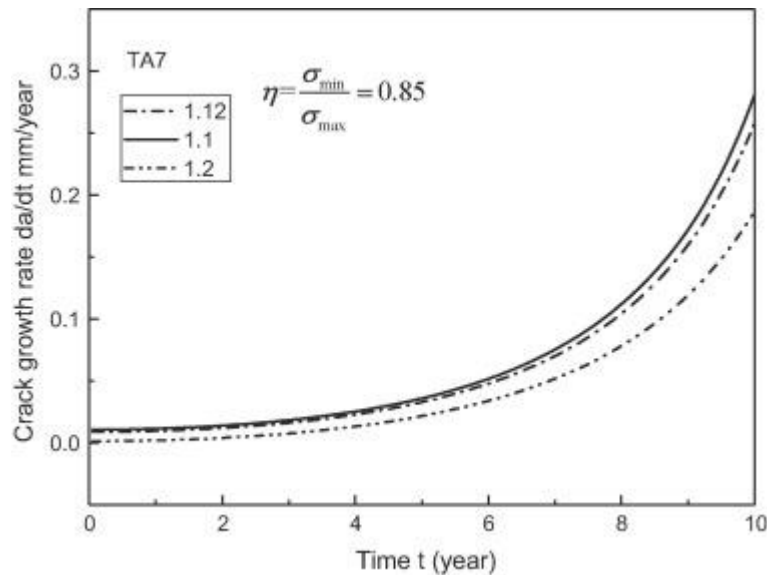
4.2. Crack growth history influenced by microscopic Poisson's ratio

The microscopic Poisson's ratio is defined as $\nu^*(t)/\nu_{\text{macro}}(T)$. The [macroscopic](#) Poisson's ratio of TA7 increases over the rise of temperature. $\nu^*(t)$ is a decaying function of t . Variation of $\nu^*(t)$ results in the change of [crack growth history](#) of titanium alloys TA7. Graphically displayed in [Fig. 10](#), [Fig. 11](#) are the crack growth history of TA7 influenced by the perturbation of coefficient in the function of $\nu^*(t)$. It can be observed that relatively higher coefficient 1.2 leads to more steady curve of crack length and crack growth rate. Nevertheless, the general trend of three curves are similar. For the sake of simplicity, $\nu_1^*(t)=-0.005t^2+1.12$ is adopted for TA7 while $\nu_2^*(t)=-0.0035t^2+1.3$ is adopted for TA19.



1. [Download high-res image \(119KB\)](#)
2. [Download full-size image](#)

Fig. 10. Variation of microscopic Poisson's ratio: Half [crack length](#) a versus time t .



1. [Download high-res image \(108KB\)](#)
2. [Download full-size image](#)

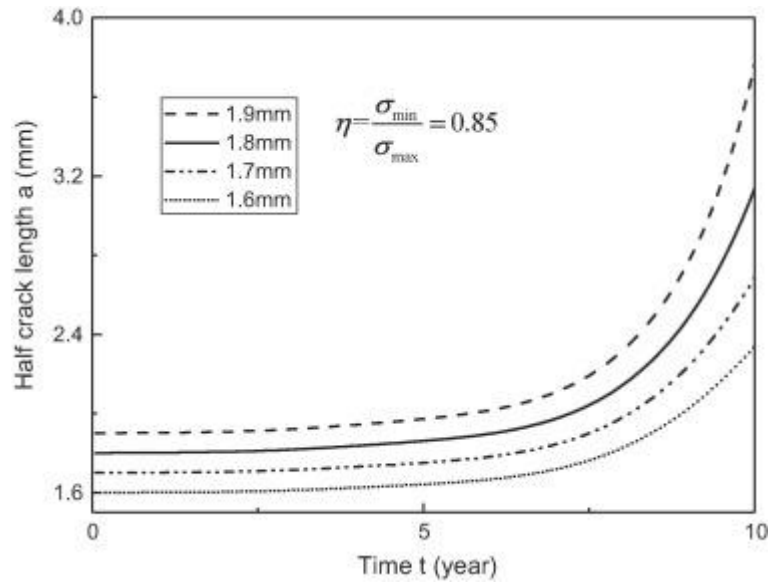
Fig. 11. Variation of microscopic Poisson's ratio: [crack growth rate](#) da/dt versus time t .

4.3. Crack growth history influenced by material differences of titanium alloys

The material differences between TA7 and TA19 can lead to vastly different crack growth history. The most prominent difference of TA7 and TA19 are the variation of macroscopic Poisson's ratio over the increase of temperature. This has been explained in last section. Other difference can be best manifested through the crack growth history of titanium alloys.

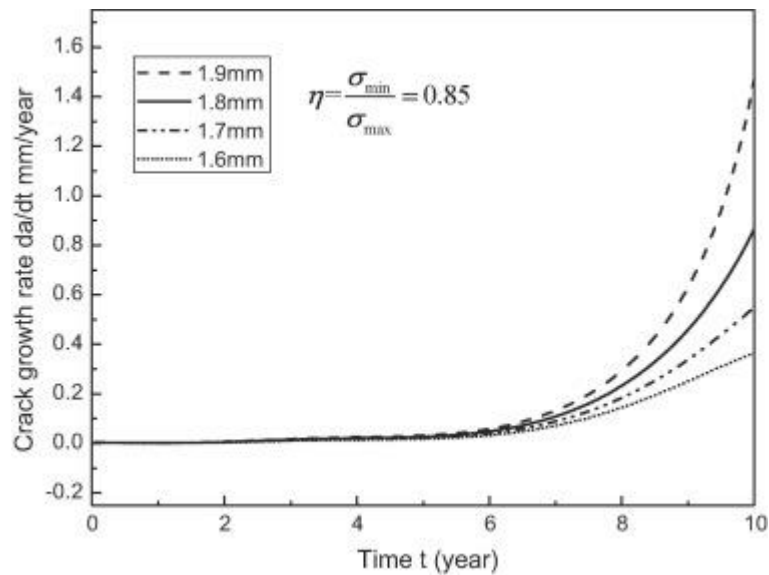
Effects of initial crack size can be critical for crack length growth and crack growth velocity. Given here is a set of initial crack lengths of 1.9 mm, 1.8 mm, 1.7 mm and 1.6 mm with a perturbation index $\eta=0.85$ under the sinusoidal temperature field of $T(t)=425+125\sin 3\pi t/10$.

Displayed in [Fig. 12](#), [Fig. 13](#) are the plots of crack growth history for titanium alloys TA7. Notice that all of the four curves in [Fig. 12](#) have not reached the critical crack length after 10 years of thermal-mechanical loading. Until 10 years of designed life expectancy, curves of crack length and crack growth rate remain steadily increasing. Slopes of these curves have not sharply changed. Therefore, from the perspective of inverse approach, the set of micro/macro scale parameters and functions are appropriate.



1. [Download high-res image \(122KB\)](#)
2. [Download full-size image](#)

Fig. 12. TA7 Half [crack length](#) a versus time t .

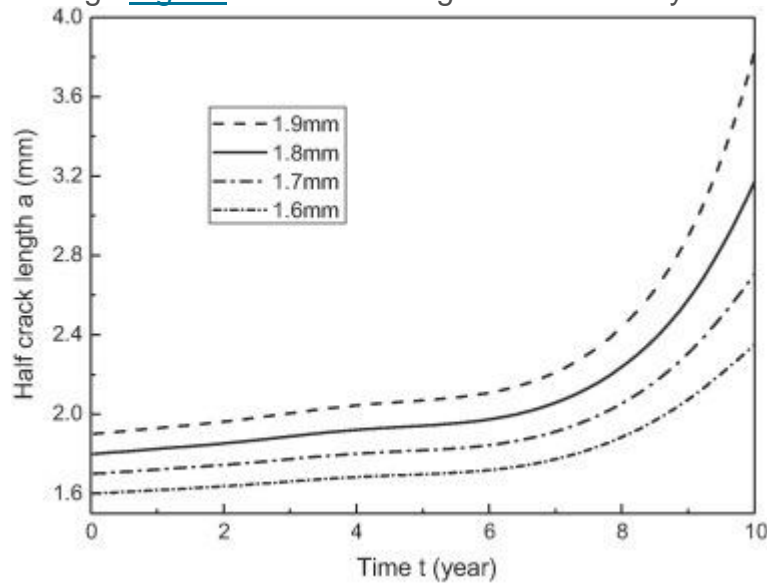


1. [Download high-res image \(117KB\)](#)
2. [Download full-size image](#)

Fig. 13. TA7: [crack growth rate](#) da/dt versus time t .

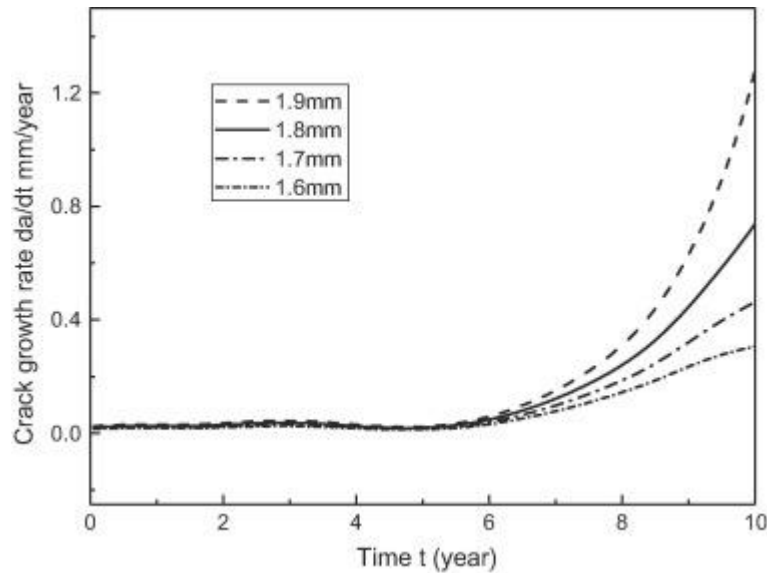
Displayed in [Fig. 14](#), [Fig. 15](#) are the plots of crack growth history for titanium alloys TA19. Similar conclusions can be made based on the curves of crack length and crack growth rate. It shall be noticed that there are slight oscillations in the curves of crack growth rate. These oscillations occur at [early stage](#) of curves. A reasonable explanation for the phenomenon is that oscillation is caused by the [sinusoidal variation](#) of

temperature field. The crack growth rate is possibly retarded by the [temperature change](#). However, the irreversible [material degradation](#) can be still reflected through [Fig. 14](#). The crack length monotonically increases over the time range.



1. [Download high-res image \(126KB\)](#)
2. [Download full-size image](#)

Fig. 14. TA19 Half [crack length](#) a versus time t .

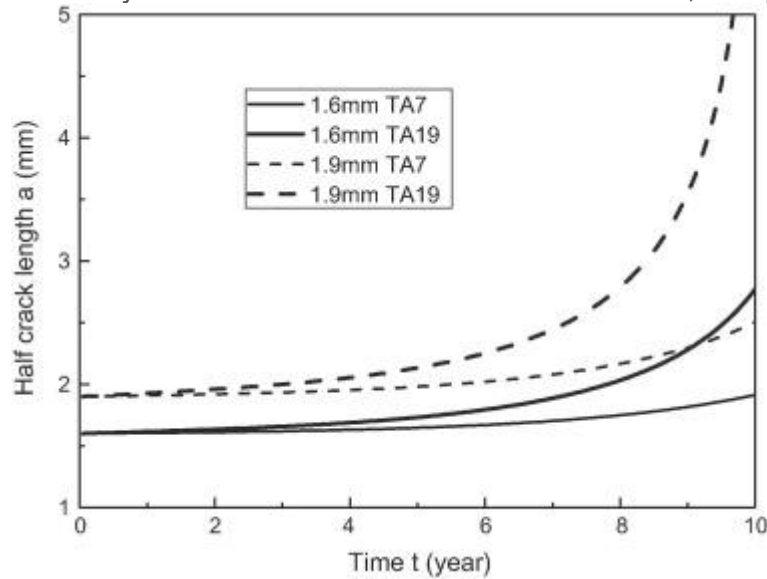


1. [Download high-res image \(106KB\)](#)
2. [Download full-size image](#)

Fig. 15. TA19: [crack growth rate](#) da/dt versus time t .

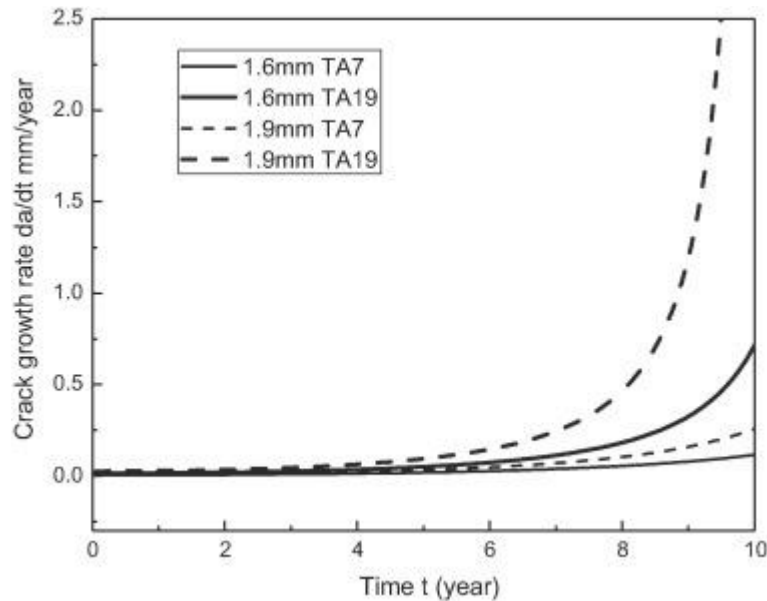
Displayed in [Fig. 16](#), [Fig. 17](#) are the composite comparison of crack length and crack growth rate for TA7 and TA19, respectively. With the same perturbation index and

temperature field, curves of TA7 tend to increase in a more conservative fashion compared to that of TA19. For initial crack length 1.9 mm of TA19, it reaches the critical crack length 4 mm around 8 years. The crack growth rate of TA19 demonstrates a sharp increase at 8 years. Therefore, it can be concluded that TA19 titanium alloys are relatively vulnerable to thermal-mechanical load, compared to TA7 titanium alloys.



1. [Download high-res image \(113KB\)](#)
2. [Download full-size image](#)

Fig. 16. Half [crack length](#) a versus time t .



1. [Download high-res image \(112KB\)](#)
2. [Download full-size image](#)

Fig. 17. [Crack growth rate](#) da/dt versus time t .

5. Concluding remarks

A dual scale [crack growth](#) model is used to study the [time-temperature](#) effects on [crack growth behaviors](#) of [titanium alloys](#) TA7 and TA19. The assessment of damage caused by creep and fatigue is explicitly expressed as an equivalent [crack length](#). Time and temperature [dependent material](#) properties of titanium alloys TA7 and TA19 are addressed. Variation of temperature field, microscopic Poisson's ratio and material difference between TA7 and TA19 are related to the crack growth behavior of titanium alloys. The main findings are summarized as follows:

1.

Time and temperature effects play substantial role in the microstructural degradation of metal materials

2.

Crack growth history is influenced by multiple factors including temperature, microscopic material properties and the difference of titanium alloys.

3.

The inverse methodology makes it possible that the optimum conditions can be determined for the desired life qualified by the initial-final defect sizes.

The inverse approach is taken on the basis of a dual crack growth model as well as experimental data of titanium alloys, though the test data is not directly related to crack growth. Our main goal is to determine the optimal time-temperature decaying parameters for the crack growth of titanium alloys. In general, this inverse methodology offers an innovative option for designers and engineers to determine the best condition for the required life according to the sizes of initial-final cracks, temperature variation and material properties. Nevertheless, these results are still preliminary and need to be further modified. One of the necessary work would be to modify and complete the dual [scale model](#). This will be left for the coming work.